INNOVARE JOURNAL OF MEDICAL SCIENCES

Vol 13, Issue 4, 2025

Online - 2321-4406
Print - 2614-5006
Research Article

SYNTHESIS, CHARACTERIZATION AND EVALUATION OF *MUCUNA PRURIENS* ZINC NANOPARTICLES: INVESTIGATING ANTI-INFLAMMATORY, ANTIOXIDANT, AND ANTI-ARTHRITIC PROPERTIES

GENEVIA FATIMA MERCY V*, KARTHIK MOHAN

Department of Biochemistry, E.G.S. Pillay Arts and Science College, Nagapattinam, Tamil Nadu, India. Email: mercyv1402@gmail.com

Received: 05 May 2025, Revised and Accepted: 25 June 2025

ABSTRACT

Objectives: The objective of the study was to synthesize zinc (Zn) nanoparticles (NPs) using *Mucuna pruriens* extract and evaluate their antioxidant, anti-inflammatory, and anti-arthritic activities through *in vitro* assays.

Methods: Zn NPs were synthesized from *M. pruriens* and subjected to a series of *in vitro* biological assays, including 2,2-diphenyl-1-picrylhydrazyl radical scavenging (antioxidant), protein denaturation inhibition, anti-proteinase activity, heat-induced hemolysis, and human red blood cell (HRBC) membrane stabilization methods (anti-inflammatory and anti-arthritic evaluations). Comparisons were made with standard reference drugs.

Results: The *M. pruriens*-derived Zn NPs demonstrated significant antioxidant, anti-inflammatory, and anti-arthritic activities. They effectively inhibited protein denaturation and stabilized red blood cell membranes, often outperforming standard drugs in the tested parameters.

Conclusion: *M. pruriens*-derived Zn NPs exhibit potent biological activities, highlighting their potential as a natural therapeutic strategy for managing oxidative stress and inflammatory diseases. Further *in vitro* and preclinical studies are recommended to confirm these findings and explore their clinical applicability.

Keywords: anti-inflammatory and anti-arthritic evaluations

 DOI: http://dx.doi.org/10.22159/ijms.2025v13i4.54160. Journal homepage: https://innovareacademics.in/journals/index.php/ijms

INTRODUCTION

In recent years, nanotechnology has garnered significant interest among researchers. The term "nanotechnology" refers to the design, synthesis, manipulation, and application of atomic or molecular structures. The engineering techniques and processes involved in creating metallic nanoparticles (NPs) modify their physical and chemical characteristics, as well as their reactivity, due to their small size and high surface-to-volume ratio [1]. Moreover, Nanomaterials exhibit atom-like behavior when reduced to near-atomic sizes, which is attributed to their large surface area and the wider bandgap between the valence and conduction bands, resulting in increased surface energy [2].

Zinc oxide (ZnO) is an inorganic compound known for its catalytic, semiconducting, piezoelectric, optoelectronic, and pyroelectric properties. ZnO NPs possess distinct characteristics such as improved light absorption and enhanced catalytic activity, attributed to their high surface area-to-volume ratio and the wide band gap between their conduction and valence bands. These NPs have been synthesized through various physical and chemical methods, including hydrothermal synthesis, vapor-liquid-solid growth, sol-gel processes, chemical vapor deposition, and microwave techniques [3,4]. ZnO has garnered significant attention as an affordable, safe, and biocompatible material, being acknowledged by the US Food and Drug Administration as the safest metal oxide. Zinc (Zn) is particularly noted for its crucial role in maintaining interactions between proteins and nucleic acids within tissues and cells. In comparison to other physiological metals like iron, cobalt, and manganese, ZnO demonstrates considerably higher chemical stability [5]. In recent years, the worldwide nanotechnology revolution with a variety of metal oxide nanomaterials, including Zn NPs has been identified, predicted to unexpected and remarkable properties in biomedical research and disease control, including drug delivery, cell imaging, antibacterial, anti-inflammatory, anti-arthritis, anti-diabetic, and cancer therapy [6-8].

Medicinal plants and herbs play a pivotal role in meeting global healthcare needs, and their importance is expected to grow in the future. Due to the side effects of chemical drugs, the use of medicinal plant extracts for treating human diseases has significantly increased over the past few decades [9]. Plants possess a wide range of therapeutic properties, including antidiuretic, antidiabetic, antiarthritic, antidepressant, antioxidant, and antibacterial effects. These properties are attributed to the presence of various bioactive compounds such as phenolics, flavonoids, alkaloids, terpenes, steroids, and saponins [10].

Plant-mediated production of NPs is a cutting-edge method with several uses in the food, pharmaceutical, and agricultural industries [11]. The nanoformulation and targeted drug delivery of this bioactive component have significantly improved its protective efficacy. *Mucuna pruriens* is a tropical twining legume, commonly known as velvet bean, belonging to the family Fabaceae [12]. It possesses numerous biological activities, including neuroprotective, antidiabetic, antioxidant, anti-epileptic, and anticancer effects. In general, nearly all parts of the *M. pruriens* plant exhibit potent medicinal properties. The primary phenolic compound in *M. pruriens* is L-DOPA, which constitutes about 3.02–4.72% of the plant [13]. Conventionally, it has been used to treat a variety of ailments, including Parkinson's disease, infertility, and snake bites, owing to its high content of L-DOPA, an important precursor to dopamine. However, the medicinal potential of *M. pruriens* extends far beyond L-DOPA, as the plant is also a rich source of phenolics, flavonoids, tannins, alkaloids, and other secondary metabolites that exhibit significant antioxidant, anti-inflammatory, and neuroprotective activities [14]. These bioactive compounds have been the focus of numerous studies aiming to elucidate the mechanisms underlying the plant's therapeutic effects. Recent research has shown that *M. pruriens* plant exhibits significant cytotoxic effects on cancer cell lines by its antioxidant capacity [15]. However, the potential of *M. pruriens* in the form of Zn NPs, particularly their efficacy in antioxidant, anti-inflammatory, and anti-arthritis, remains largely unexplored.

In this study, we describe the synthesis of ZnO NPs using a biological method involving ZnO, and an extract from the *M. pruriens* plant. The primary purpose of this research is to synthesize and characterize *M. pruriens* Zn NPs and evaluate their potential therapeutic applications, focusing on their antioxidant, anti-inflammatory, and anti-arthritic activities. The rationale for focusing on these specific applications stems from the extensive evidence supporting the role of oxidative stress and inflammation in the pathogenesis of chronic inflammatory diseases, including arthritis and other stress-related disorders. By targeting these fundamental processes, MP-ZnNPs have the potential to offer a multifaceted approach to disease treatment.

METHODS

Chemicals

Chemicals used in the study were ascorbic acid, gallic acid, tannic acid, catechol, butylated hydroxyl toluene, Folin-Ciocalteau reagent, 2,2-diphenyl-1-picrylhydrazyl radical (DPPH), sodium carbonate, sodium nitrite, aluminum chloride, sodium hydroxide, potassium ferric cyanide, ferric chloride, sodium phosphate, ammonium molybdate, ferrous ammonium sulphate, ethylenediaminetetraacetic acid, dimethyl sulphoxide (DMSO), ammonium acetate, nicotinamide adenine dinucleotide, nitro blue tetrasolium, phenazine methosulphate, hydrogen peroxide, sodium nitroprusside (SNP), sulphanilamide, naphthyethylene diamine dihydrochloride, glacial acetic acid, acetyl acetone, sulfuric acid, phosphoric acid, trichloroacetic acid (TCA), and ferrozine. All the chemicals were purchased from and all solvents used were of analytical grade.

Phytochemical analysis

Twenty grams of dried plant stems were mixed with 200 mL of deionized water and shaken for 30 min in a water bath at 70°C. The resulting extract was filtered, and the filtrate was stored at 4°C for further use. The total phenolic, flavonoid, saponin, alkaloid, and tannin contents of the aqueous extract of *M. pruriens* stems were quantitatively estimated.

Assessment of flavonoids

Add 1–2 mL of methanol to 0.5 g of the sample. Filter the mixture through filter paper. Transfer the filtrate to a crucible, evaporate it to dryness using a water bath, and then weigh the residue.

Assessment of tannin

Mix 0.5 g of the sample with 1 mL of distilled water. Filter the solution, then add 1 drop of ferric chloride and 1 drop of potassium ferrocyanide to the filtrate. Dry the resulting sample in a crucible until it reaches a constant weight after evaporation.

Assessment of saponin

Combine 1 mL of diethyl ether with 0.5 g of the sample. Shake vigorously and filter to separate the solution into two layers. Remove the upper layer, then add 1 drop of n-butanol and 1 drop of NaCl. Heat the mixture in a water bath, then dry the sample in a crucible to a constant weight after evaporation.

Assessment of alkaloids

Add a solution of 10% acetic acid in ethanol (100 µL of acetic acid in 900 µL of ethanol) to 0.5 g of the sample. Filter the solution, then add 1 drop of ammonia solution to the filtrate. Dry the sample and record the weight.

Assessment of phenol

Add 1 mL of distilled water to 0.5 g of the sample and filter the solution. To the filtrate, add 1 drop each of ammonia solution and isoamyl alcohol. Dry the sample in a crucible until it reaches a constant weight after evaporation.

Nanoparticle synthesis and characterization

Preparation of metal NPs

Dissolve Zn nitrate hexahydrate in deionized water to create a 2 mM Zn nitrate solution, and the solution was added gradually in portions to a well-stirred plant extract as the reducing agent (*M. pruriens*) to this solution with continuous stirring. The color change and the appearance of a white precipitate indicate the formation of Zn NPs. Filter and wash the precipitate to remove impurities, and then dry it to obtain Zn NPs.

Structure characterization of the metal NPs

UV-Visible analysis

The optical properties of ZnO NPs were characterized using ultraviolet-visible spectroscopy (UV-VIS) Spectra. The color change was observed from transparent white to light sandal indicated the presence of ZnO NPs. The absorbance was recorded between 350 nm and 500 nm by UV after 24 h of addition [16].

Fourier transform infrared (FTIR) analysis

Fourier transform infrared spectroscopy is also known as FTIR spectroscopy or FTIR analysis. The synthesized ZnO NPs can be scanned by infrared light, and chemical properties such as polymeric organic and inorganic materials were detected by FTIR. It absorbs within the range of 400–4000 cm^{-1}. Multiple functional groups may be absorbed at a particular frequency, and it gives rise to different characteristic absorptions [17].

X-ray diffraction (XRD)

The structural of nanomaterials (range of 1–100 nm) can be study by using XRD analysis. The position of values of product (amorphous or crystallinity nature) can be observed by XRD. The fingerprint regions of relative intensity are found in XRD analysis with respect to d-spacing values [18].

Scanning electron microscopy (SEM) analysis

SEM analysis of synthesized ZnO NPs was performed to evaluate the surface morphology of NPs. ZnO NPs were prepared and dried to eliminate the moisture content and images were taken by using FEI Quanta 250 SEM operating at 10 Kv [19].

Energy dispersive X-ray analysis (EDAX)

Analysis through EDAX spectrometer proved that ZnO NPs is present. The horizontal axis shows energy in keV, whereas the vertical axis shows the number of X- ray counts [20].

Antioxidant activity

DPPH assay method

The antioxidant activity of the *M. pruriens* extract and synthesized ZnO NPs was determined using the DPPH free radical scavenging assay according to the method described by [21]. Briefly, 1 mL of DPPH solution (0.1 mM in methanol) was mixed with 1 mL of different concentrations of the plant extract or NPs (10, 20, 40, 60, 80, and 100 µg/mL). The mixture was incubated in the dark for 30 min at room temperature. Ascorbic acid is used as the standard drug. The absorbance was measured at 517 nm using a UV-Vis spectrophotometer. The percentage of DPPH radical scavenging activity was calculated using the formula:

$$\text{Scavenging Activity (\%)} = (A_{control} - A_{sample}/A_{control}) \times 100.$$

Where A control is the absorbance of the control reaction (DPPH solution without sample) and A sample is the absorbance of the test sample.

Scavenging of 2,2′-azino-bis(3-ethylbenzothiazoline-6-sulfonic acid) (ABTS) radical cation

To 1 mL of different concentrations of the extract or standard (ascorbic acid), 1.0 mL of distilled DMSO, and 3 mL of ABTS solution were added

and incubated for 20 min. The absorbance of the resulting solutions was measured spectrophotometrically at 734 nm [22]. The percentage of inhibition was calculated using the following formula:

$$\% \text{ Inhibition} = \{\text{Control–Test}\}/\{\text{Control}\}\} \times 100$$

Scavenging of hydrogen peroxide

A hydrogen peroxide solution (20 mM) was prepared in phosphate-buffered saline ([PBS], pH 7.4). To 2 mL of the hydrogen peroxide solution in PBS, 1 mL of various concentrations of *M. pruriens* extract and synthesized ZnO NPs or standard ascorbic acid (20–100 µg/mL) in ethanol was added. After 10 min, the absorbance was measured at 230 nm [23].

$$\% \text{ inhibition} = ([\text{Control–Test}]/\text{control}) \times 100$$

Ferric reducing antioxidant power (FRAP)

Different concentrations of the samples (20–100 µg/mL) were added to 2.5 mL of 0.2 M sodium phosphate buffer (pH 6.6) and 2.5 mL of 1% potassium ferricyanide ($K_3Fe[CN]_6$) solution. The reaction mixture was thoroughly vortexed and then incubated at 50°C for 20 min using a vortex shaker. After incubation, 2.5 mL of 10% TCA was added to the mixture and centrifuged at 3,000 rpm for 10 min. The supernatant (2.5 mL) was then mixed with 2.5 mL of deionized water and 0.5 mL of 0.1% ferric chloride. The absorbance of the resulting colored solution was measured at 700 nm using a UV spectrophotometer, with a blank serving as the reference [24]. Ascorbic acid was used as a reference standard, and the results were compared with this standard.

$$\% \text{ inhibition} = ([\text{Control–Test}]/\text{control}) \times 100$$

Nitric oxide radical scavenging activity (NORS)

The activity was assessed using a standard method. To 0.5 mL of the extract at various concentrations (10–200 µg/mL), 1 mL of SNP solution (5 mM) in 0.1 M PBS (pH 7.4) was added and incubated at room temperature for 30 min. After incubation, 1.5 mL of Griess reagent (1% sulfanilamide in 5% phosphoric acid and 0.1% naphthylethylenediamine dihydrochloride) was added, and the mixture was incubated for an additional 15 min at room temperature. The absorbance of the samples was immediately measured at 546 nm and compared with the standard, ascorbic acid [25].

$$\% \text{ inhibition} = ([\text{Control–Test}]/\text{control}) \times 100$$

Anti-inflammatory activity

Inhibition of albumin denaturation

The reaction mixture contained 1 mL of egg albumin, 1 mL of various concentrations of the sample (20–100 µg/mL), and 1 mL of (PBS, pH 6.4). The mixture was incubated at 37°C for 15 min, followed by heating at 70°C for 5 min. After cooling, the absorbance of the samples and the standard drug, diclofenac sodium, was measured at 660 nm using a spectrophotometer. The percentage inhibition of protein denaturation was calculated [26].

Percentage inhibition of proteinase activity

The reaction mixture consisted of 1 mL of 0.06 mg trypsin, 1 mL of Tris-HCl buffer (pH 7.4), and 1 mL of various concentrations of the sample (20–100 µg/mL). The mixture was incubated at 37°C for 5 min, followed by the addition of 1 mL of 0.8% (w/v) casein. After further incubation for 20 min, 1 mL of 70% perchloric acid was added to stop the reaction. The cloudy suspension was centrifuged, and the absorbance of the supernatant was measured at 210 nm. The percentage inhibition of proteinase activity was calculated.

Percentage membrane stabilizing activity by heat-induced hemolysis

The mixture in each test tube consisted of 1 mL of hyposaline (0.25% w/v sodium chloride), 1 mL of 0.15 M phosphate buffer (pH 7.4), 1 mL of the sample at concentrations of 20–100 µg/mL, and 0.5 mL of 10% human red blood cells (HRBCs) in isosaline. The test control consisted of 1 mL of distilled water. The reaction mixture and the standard drug, diclofenac sodium, were each incubated for 30 min at 37°C and then centrifuged at 3,000 rpm for 20 min. The hemoglobin content in the suspension was estimated using a spectrophotometer at 560 nm. The percentage of membrane stabilizing activity was calculated.

Percent inhibition of lipoxygenase activity

The reaction mixture consisted of 1 mL of the sample or standard drug indomethacin at concentrations of 20–100 µg/mL, 0.25 mL of 2 M borate buffer (pH 9.0), and 0.25 mL of lipoxygenase enzyme solution (20,000 U/mL). The mixture was incubated for 5 min at 25°C. Afterward, 1 mL of linoleic acid solution (0.66 mM) was added to the test sample, mixed thoroughly, and the absorbance was measured at 234 nm. The percent inhibition was calculated using the formula:

$$\% \text{ inhibition} = \frac{\text{Abs control- Abs treated}}{\text{Abs control}} \times 100$$

Where, Abs control = absorbance of control, Abs treated = absorbance of test sample.

Anti-arthritis activity

Inhibition of protein denaturation model

Egg albumin (0.2 mL), (PBS, pH 6.4, 2.8 mL), and various concentrations of sample (20–100 µg/mL) were prepared as test solutions. Diclofenac sodium served as the standard drug. All solutions were adjusted to pH 6.4, incubated at 37°C for 15 min, then heated at 70°C for 5 min. After cooling, absorbance was measured at 660 nm, and the percentage inhibition of protein denaturation was calculated.

$$\text{Percentage inhibition} = (Vc/Vt-1) \times 100$$

Where Vt is the absorbance of the test sample, and Vc is the absorbance of the control.

Assay of membrane stabilizing activity

The test solution contained 1 mL phosphate buffer, 2 mL hyposaline, 0.5 mL HRBC suspension, and various concentrations of the sample (20–100 µg/mL). Diclofenac sodium served as the standard. All mixtures were incubated at 37°C for 30 min, centrifuged at 3000 rpm, and the hemoglobin content was measured at 560 nm. The percentage of membrane stabilization was calculated relative to the control.

$$\% \text{ Membrane stabilization} = (\text{Absorbance of control} - \text{Absorbance of sample}) \times 100$$

Where: Absorbance of control is the absorbance of the hemolysis solution without any treatment. Absorbance of sample is the absorbance of the solution treated with the sample or standard drug.

Gas chromatography-mass spectroscopy (GC-MS) analysis of aqueous extract of *M. pruriens*

Dried *M. pruriens* seeds were finely powdered, and 10 g of the powder was extracted in 100 mL of distilled water by refluxing at 60°C for 2 h. The extract was filtered using Whatman No.1 filter paper and lyophilized to obtain a dry residue. The dried extract was reconstituted in high-performance liquid chromatography grade methanol for analysis. GC-MS analysis was performed using an Agilent 7890A GC system equipped with a 30 m × 0.25 mm × 0.25 µm DB-5 capillary column. Initially, the instrument was maintained at 100°C for 2.1 min. The temperature was then increased to 300°C at a rate of 25°C/min and held for 10 min. The injection port temperature was set at 250°C, and helium was used as the carrier gas at a flow rate of 1.5 mL/min. Mass spectrometry (MS) was conducted in electron ionization mode (70 eV), with the *M. pruriens* extract injected in split mode (5:1). The MS scan range was set to 35–900 m/z. The fragmentation patterns

of the detected compounds were compared with those stored in the W8N05ST Library MS database for identification. The percentage of each compound was calculated based on its relative peak area in the chromatogram using ChemStation integrator algorithms.

Statistical analysis
All experiments were performed in triplicates, and data are presented as mean±standard deviation. The IC_{50} values were determined using nonlinear regression analysis in GraphPad Prism.

RESULTS AND DISCUSSION

Quantitative analysis of secondary metabolites in *M. pruriens* plant extract
The quantitative analysis of secondary metabolites in the *M. pruriens* plant extract was conducted to determine the presence and concentration of various bioactive compounds, including flavonoids, tannins, saponins, alkaloids, phenols, and terpenoids (Table 1). The analysis revealed the following concentrations (expressed as mg per Gram of sample):

Flavonoids were the most abundant compound in the extract, with a concentration of 0.032 mg/g, indicating their major role in antioxidant activity. Terpenoids followed at 0.027 mg/g, likely contributing to anti-inflammatory effects. Tannins (0.017 mg/g) and phenols (0.014 mg/g) were also present, supporting antioxidant and anti-inflammatory potential. Saponins (0.011 mg/g) and alkaloids (0.009 mg/g) were detected in lower amounts but are significant for their immune-boosting, cholesterol-lowering, and therapeutic properties. These findings highlight *M. pruriens*' potential as a source of bioactive compounds with diverse therapeutic benefits.

Synthesis and characterization of ZnO NPs using *M. pruriens* extract
The synthesis of ZnO NPs was successfully achieved using a green synthesis method involving *M. pruriens* plant extract as a reducing and stabilizing agent. Zn nitrate was used as the precursor for Zn ions. The synthesis process was characterized by a color change in the reaction mixture, indicating the formation of ZnO NPs.

Visual observation
The reaction mixture initially appeared pale yellow due to the Zn nitrate solution. Upon the addition of *M. pruriens* extract, the solution gradually turned turbid, with a distinct white precipitate forming over time, suggesting the formation of ZnO NPs.

UV-Vis spectroscopy
The UV-Vis absorption spectrum of the synthesized ZnO NPs showed a characteristic peak at around 279 nm, confirming the presence of ZnO NPs. This peak corresponds to the intrinsic band-gap absorption of ZnO due to electron transitions from the valence band to the conduction band (Fig. 1a)

XRD analysis
XRD analysis of the synthesized ZnO NPs revealed distinct diffraction peaks at 2θ values corresponding to the hexagonal wurtzite structure of ZnO. The peaks were sharp and well-defined, indicating the crystalline nature of the NPs. The average crystallite size was calculated using the Debye-Scherrer formula and found to be in the range of 20–30 nm (Fig. 1b).

Table 1: Quantitative analysis of secondary metabolites in *Mucuna pruriens* plant extract

S. No.	Phytochemical constituents	Sample (mg/g)
1.	Flavonoids	0.032
2.	Tannin	0.017
3.	Saponins	0.011
4.	Alkaloids	0.009
5.	Phenol	0.014
6.	Terpenoids	0.027

Energy dispersive X-ray spectroscopy (EDS)
EDS analysis confirmed the elemental composition of the synthesized NPs, showing strong signals corresponding to Zn and oxygen (O), with no significant impurities. This purity further validates the effectiveness of the green synthesis method using *M. pruriens* extract (Fig. 1c).

SEM
SEM images showed that the ZnO NPs were predominantly spherical in shape with a uniform size distribution. The NPs appeared to be well-dispersed, with minimal agglomeration, indicating the effectiveness of the *M. pruriens* extract as a stabilizing agent (Fig. 2).

Antioxidant activity of *M. pruriens* extract
DPPH assay method
The antioxidant activity of *M. pruriens* coated with Zn NPs and ascorbic acid is presented in the results. The DPPH scavenging activity of the *M. pruriens*-coated Zn NPs and ascorbic acid was evaluated at five different concentrations (20–100 µg/mL). The observed activity ranged from 44.73% to 71.92% for the *M. pruriens* sample and 48.24–78.94% for ascorbic acid. The IC_{50} values were 37.90±0.01 µg/mL for the *M. pruriens* sample and 27.60±0.03 µg/mL for ascorbic acid.

Scavenging of ABTS radical cation
The ABTS radical cation scavenging activity of *M. pruriens* coated with Zn NPs and ascorbic acid was assessed at various concentrations (20–100 µg/mL). The activity ranged from 40.90% to 70.90% for the *M. pruriens* sample and 47.27–81.81% for ascorbic acid. The IC_{50} values were 41.51 µg/mL for the *M. pruriens* sample and 23.36 µg/mL for ascorbic acid.

Scavenging of hydrogen peroxide
The hydrogen peroxide scavenging activity of *M. pruriens* coated with Zn NPs and ascorbic acid was assessed at concentrations ranging from 20 to 100 µg/mL. Ascorbic acid exhibited higher scavenging activity, ranging from 50.48% to 76.69%, compared to the *M. pruriens* sample, which ranged from 38.83% to 64.07%. The IC_{50} values were 20.33 µg/mL for ascorbic acid and 55.56 µg/mL for the *M. pruriens* sample, indicating that while *M. pruriens*-coated Zn NPs are less effective than ascorbic acid, they still possess significant antioxidant activity.

FRAP
The antioxidant activity of *M. pruriens* coated with Zn NPs and ascorbic acid was evaluated using the FRAP method at various concentrations (20–100 µg/mL). Ascorbic acid showed antioxidant activity ranging from 49.10% to 81.25%, whereas the *M. pruriens* sample ranged from 43.75% to 69.64%. The IC_{50} values were 20.05 µg/mL for ascorbic acid and 36.16 µg/mL for the *M. pruriens* sample.

NORS
The scavenging activity of *M. pruriens* coated with Zn NPs and ascorbic acid against nitric oxide radicals was tested at concentrations from 20 to 100 µg/mL. Ascorbic acid demonstrated scavenging activity ranging from 47.11% to 82.69%, while the *M. pruriens* sample ranged from 39.42% to 72.11%. The IC_{50} values were 28.67 µg/mL for ascorbic acid and 46.12 µg/mL for the *M. pruriens* sample.

These results indicate that *M. pruriens*-coated ZnO NPs have notable antioxidant potential, though they are somewhat less effective compared to ascorbic acid (Fig. 3a-e).

Anti-inflammatory activity of *M. pruriens* extract with ZnO NPs
The anti-inflammatory effects of *M. pruriens*-coated Zn NPs were evaluated and compared with Diclofenac sodium using three different

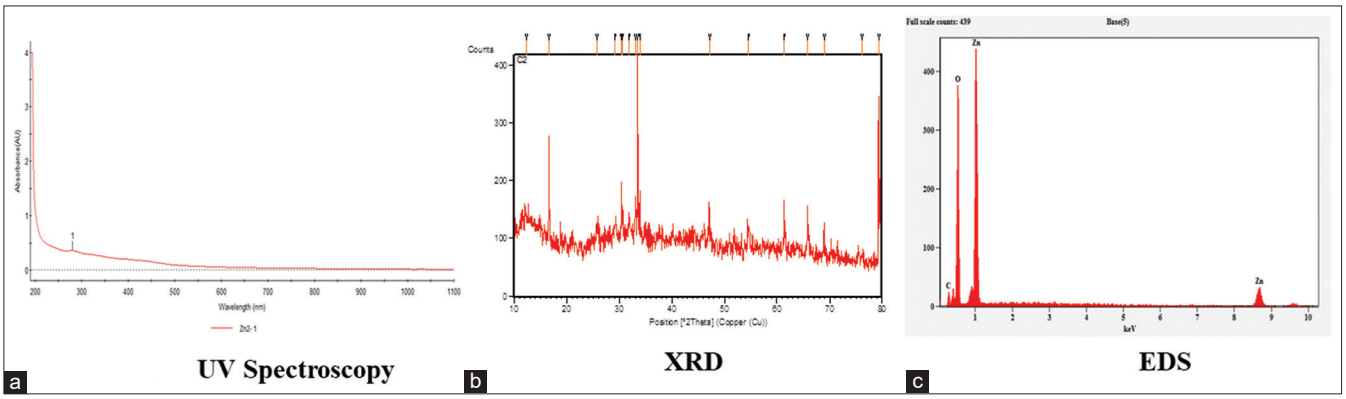

Fig. 1: Characterizations of zinc nanoparticles with ultraviolet-visible spectroscopy (a), X-ray diffraction (b) and energy dispersive X-ray spectroscopy (c)

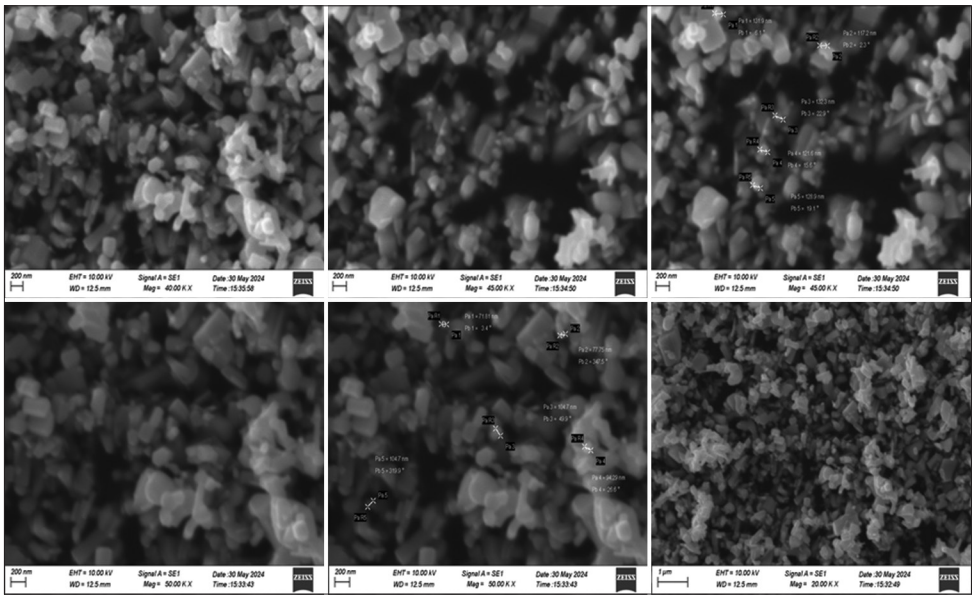

Fig. 2: Scanning electron microscopy images of zinc nanoparticles under ×200 magnification

methods: Protein denaturation, anti-proteinase action, and heat-induced hemolysis.

Protein denaturation method

M. pruriens-coated Zn NPs demonstrated inhibition of protein denaturation ranging from 40.17% to 66.96% at concentrations between 20 µg/mL and 100 µg/mL. Diclofenac sodium showed higher inhibition, from 48.21% to 81.25% in the same range. The IC_{50} value for the *M. pruriens* sample was 53.60 µg/mL, compared to 27.85 µg/mL for Diclofenac sodium. This indicates that while *M. pruriens*-coated Zn NPs exhibit significant anti-inflammatory potential, Diclofenac sodium remains more effective.

Anti-proteinase action method

The *M. pruriens*-coated Zn NPs exhibited anti-proteinase activity between 44.14% and 70.27% across the concentrations of 20–100 µg/mL. Diclofenac sodium showed activity ranging from 48.64% to 79.27%. The IC_{50} value for *M. pruriens* was 36.73 µg/mL, whereas Diclofenac sodium had an IC_{50} value of 27.25 µg/mL. This demonstrates that *M. pruriens*-coated Zn NPs have notable anti-proteinase activity, though Diclofenac sodium is more effective.

Heat-induced hemolysis method

In the heat-induced hemolysis assay, *M. pruriens*-coated Zn NPs provided inhibition of hemolysis between 44.06% and 67.79% at concentrations from 20 to 100 µg/mL. Diclofenac sodium exhibited inhibition from 49.15% to 83.05%. The IC_{50} value for *M. pruriens* was 43.54 µg/mL, while Diclofenac sodium had an IC_{50} value of 36 µg/mL. These results suggest that *M. pruriens*-coated Zn NPs offer significant protection against heat-induced hemolysis, though Diclofenac sodium shows higher efficacy.

Overall, M. pruriens-coated ZnO NPs demonstrate substantial anti-inflammatory activity in protein denaturation, anti-proteinase, and heat-induced hemolysis methods, with effectiveness closely approaching that of Diclofenac sodium (Fig. 4a-c).

Anti-arthritic activity of *M. pruriens* extract

Inhibition of protein denaturation method

The anti-arthritic activity of *M. pruriens* Zn NPs was evaluated using the inhibition of protein denaturation method, with diclofenac sodium as the standard drug. The results showed a concentration-dependent increase in protein denaturation inhibition for both the sample and the standard drug. At the lowest concentration of 20 µg/mL, the sample exhibited a 42.47% inhibition, while diclofenac sodium showed a higher inhibition of 48.67%. As the concentration increased, the inhibition percentages also increased, with the sample achieving 73.45% inhibition at 100 µg/mL, compared to 80.53% for diclofenac sodium. The IC_{50} value for the sample was calculated to be 54.35 µg/mL, while for diclofenac sodium, it was significantly lower at 27.31 µg/mL. These

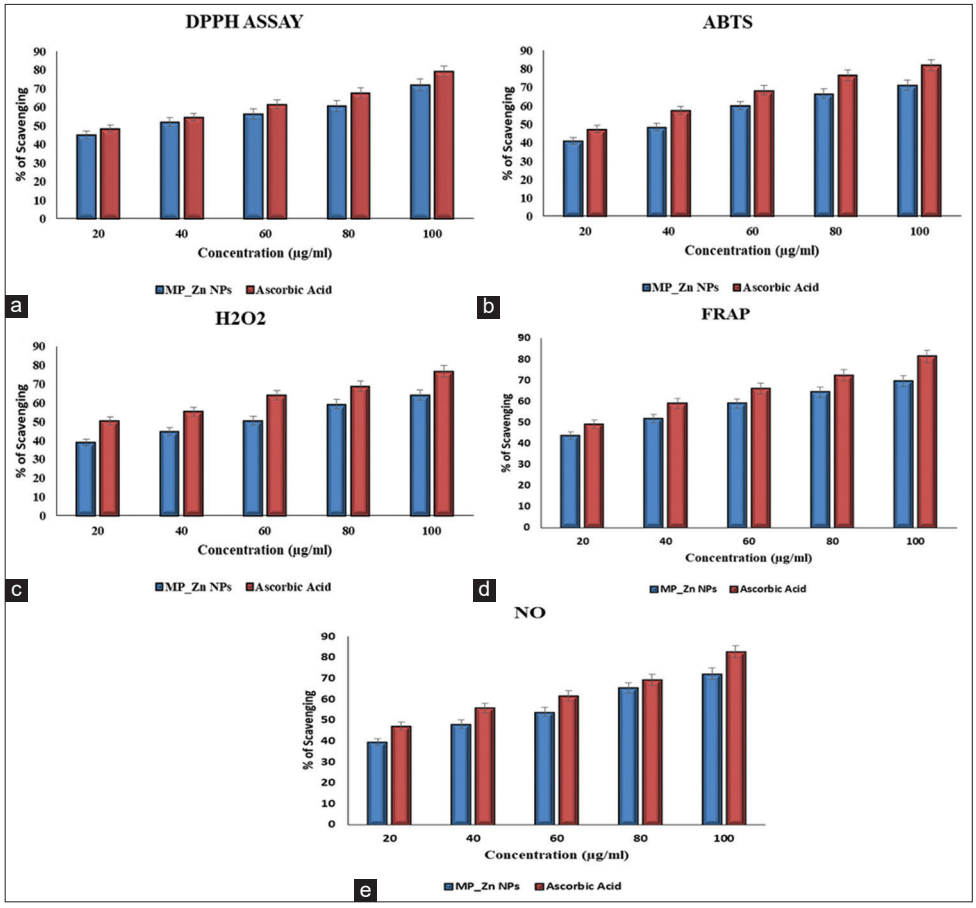

Fig. 3: Antioxidant activity of *Mucuna pruriens* zinc nanoparticles with 2,2-diphenyl-1-picrylhydrazyl assay (a), 2,2′-azino-bis(3-ethylbenzothiazoline-6-sulfonic acid) (b), H_2O_2 (c), ferric reducing antioxidant power (d) and NO assay (e). Ascorbic acid used as standard drug

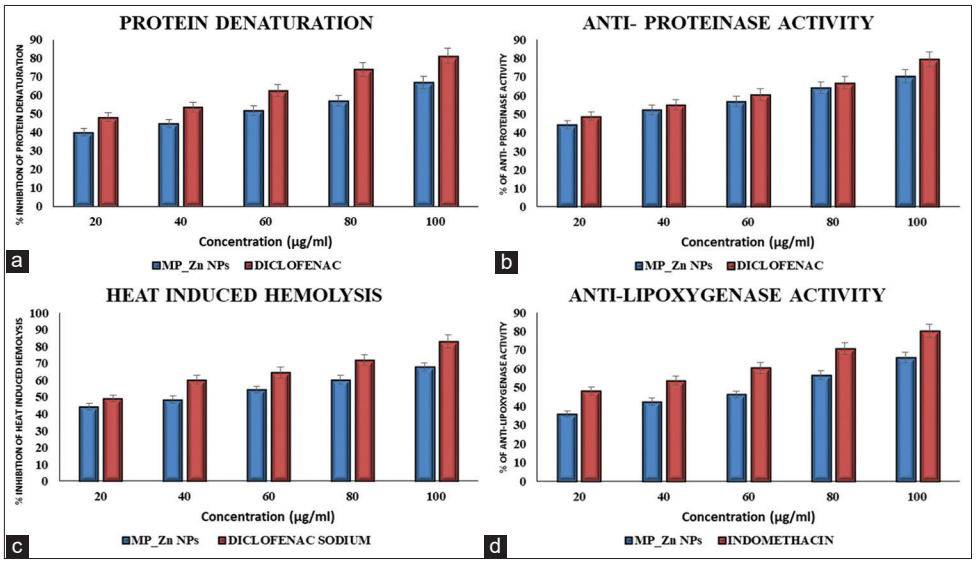

Fig. 4: Anti-inflammatory activity of *Mucuna pruriens* zinc nanoparticles with protein denaturation (a), anti-proteinase (b) and heat induced hemolysis assay (c) and anti-lipoxygenase activity (d). Diclofenac sodium and indomethacin used as standard drug

results indicate that while the *M. pruriens* Zn NPs exhibit significant anti-arthritic activity, diclofenac sodium remains more potent in this assay.

HRBC membrane stabilization method

The anti-arthritic activity of *M. pruriens* Zn NPs was evaluated using the HRBC membrane stabilization method, comparing the results with those of the standard drug diclofenac sodium. At a concentration of 20 µg/mL, the sample demonstrated a 38.79% stabilization of the HRBC membrane, while diclofenac sodium achieved 44.82%. As the concentration increased, the stabilization effect of both the sample and the standard improved. At 100 µg/mL, the sample showed a stabilization percentage of 62.93%, compared to 81.03% for

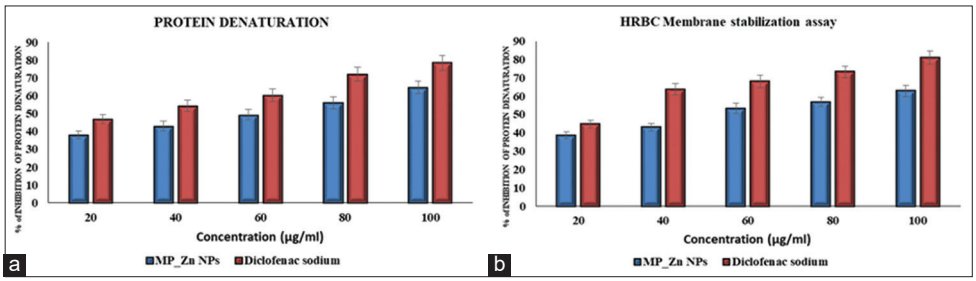

Fig. 5: Anti-arthritis activity of *Mucuna pruriens* zinc nanoparticles with protein denaturation (a) and human red blood cell assay (b). Diclofenac used as standard drug

Table 2: A typical GC-MS chromatogram of the chemical compounds of the aqueous extract of *Mucuna pruiens* (above 1% area of GC-MS)

Peak	Retention time	Area	Area %	Height	Height%	A/H	Name
1	13.857	13538	8.9	8656	10.92	1.56	Cyclohexasiloxane, dodecamethyl-
2	32.874	31042	20.4	13376	16.88	2.32	BIS (2-Ethylhexyl) ester of hexanedioic acid
3	38.765	6314	4.15	3702	4.67	1.71	2-ferrocenyl-4,4-dimethyloxazoline
4	38.855	12897	8.48	3945	4.98	3.27	(3.alpha., 4a.beta., 5.beta., 8a.alpha.)-(+-)-3,4,4A,5,6,7,8,8A-octahydro-3-hydroxy-4a, 7,7-trimethyl-5-[[(1,1-dimethylethyl) dimeth
5	38.876	3221	2.12	4264	5.38	0.76	20-deethyl-2,16-dihydro-17.alpha.-hydroxy-1-(p-tolsulfonyl) aspidospermidine
6	39.06	11401	7.49	5660	7.14	2.01	Cyclotetrasiloxane, octamethyl-
7	39.114	4719	3.1	4996	6.3	0.94	Tetrasiloxane, 1,1,3,3,5,5,7,7-octamethyl-
8	39.155	8100	5.32	4461	5.63	1.82	Pentasiloxane, 1,1,3,3,5,5,7,7,9,9-decamethyl-
9	39.206	3271	2.15	4645	5.86	0.7	Benzeneacetic acid, .alpha.,4-bis[(trimethylsilyl) oxy]-, trimethylsilyl ester
10	39.27	14364	9.44	4315	5.44	3.33	3-Carbazolyl methyl ketone thiosemicarbazone
11	39.43	5711	3.75	4094	5.17	1.39	3-Carbazolyl methyl ketone thiosemicarbazone
12	39.747	9127	6	3807	4.8	2.4	2-Furancarboxamide, N-(4-bromophenyl)-
13	39.937	12709	8.35	4311	5.44	2.95	Anthracene, 9-[2-(1,1-dimethylethoxy) ethyl]-10-phenyl-
14	40.164	8451	5.55	4755	6	1.78	4,4-dimethyl-2-(2-hydroxy-6-methoxy-3,4-(methylenedioxy) phenyl)-2-oxazoline
15	40.187	7307	4.8	4269	5.39	1.71	2-oxa-3-oxo-7-(3,8-di (trimethylsiloxy)-1-octenyl)-8-(trimethylsiloxy) bicyclo[4.3.0]nonane

GC-MS: Gas chromatography-mass spectroscopy

diclofenac sodium. The IC_{50} value for the sample was calculated to be 56.77 µg/mL, which was higher than the IC_{50} of 20.46 µg/mL for diclofenac sodium. This data indicates that while *M. pruriens* Zn NPs exhibit substantial anti-arthritic effects, the potency is less than that of diclofenac sodium as indicated by the HRBC membrane stabilization method (Fig. 5a and b).

Compounds identification from MP through GC-MS analysis

The chemical composition of the *M. pruriens* aqueous extract was identified using GC-MS analysis. A total of 15 compounds were detected in the GC-MS spectrum, accounting for 94.84% of the total aqueous extract (Table 2). Specifically, 10 compounds were documented based on their relative peak area (above 1%), contributing to 93.73% of the total peak area. These identified compounds are considered the major bioactive constituents of *M. pruriens*, potentially responsible for its anti-inflammatory, antioxidant, and anti-arthritic properties.

CONCLUSION

Redox homeostasis, a key factor in sustaining healthy cellular function, depends on the delicate balance between pro-oxidant production and the corresponding antioxidant defense system [27]. An imbalance, characterized by excessive reactive oxygen species or diminished antioxidant capacity, is a common feature in chronic inflammatory diseases. Plants with antioxidant properties, and their derived NPs, are emerging as promising strategies to counteract oxidative stress and related conditions such as inflammation and arthritis. In this study, we synthesized Zn NPs derived from *M. pruriens* and evaluated their activity focusing on anti-inflammatory, antioxidant, and anti-arthritic effects. Our findings demonstrate that these plant-derived Zn NPs exhibit significant efficacy in all tested activities when compared to standard drugs. This underscores the potential medicinal value of *M. pruriens*, suggesting it as a viable candidate for further validation in both *in vitro* and preclinical studies. Such research could contribute valuable insights into alternative strategies for managing oxidative stress and inflammatory diseases.

AUTHORS CONTRIBUTION

Genevia: Writing - Original Draft, validation, formal analysis
Karthik: Writing - Review and Editing, conceptualization, investigation

CONFLICTS OF INTEREST

The authors want to declare that there are no conflict of interests in this article.

FUNDING

No fundings were acquired for this research work.

REFERENCES

1. Huang Q, Yu H, Ru Q. Bioavailability and delivery of nutraceuticals using nanotechnology. J Food Sci 2010;75:R50-7.
2. Sahoo S. Socio-ethical issues and nanotechnology development: Perspectives from India. In: 10th IEEE International Conference on Nanotechnology. 2010. p. 1205-10.
3. Sirelkhatim A, Mahmud S, Seeni A, Mohamad Kaus NH, Ann LC, Mohd Bakhori SK, *et al*. Review on zinc oxide nanoparticles: Antibacterial activity and toxicity mechanism. Nano-Micro Lett 2015;7:219-42.
4. Wang ZL. Zinc oxide nanostructures: Growth, properties and applications. J Phys Condens Matter 2004;16:R829.
5. Naseer M, Aslam U, Khalid B, Chen B. Green route to synthesize zinc oxide nanoparticles using leaf extracts of *Cassia fistula* and melia

azadarach and their antibacterial potential. Sci Rep 2020;10:9055.
6. Anjum S, Hashim M, Asad Malik S, Khan M, Lorenzo JM, Abbasi BH, *et al*. Recent advances in zinc oxide nanoparticles (ZnO NPs) for cancer diagnosis, target drug delivery, and treatment. Cancers 2021;13:4570.
7. Merugu R, Gothalwal R, Deshpande PK, De Mandal S, Padala G, Latha Chitturi K. Synthesis of Ag/Cu and Cu/Zn bimetallic nanoparticles using toddy palm: Investigations of their antitumor, antioxidant and antibacterial activities. Mater Today Proc 2021;44:99-105.
8. Agarwal H, Shanmugam V. A review on anti-inflammatory activity of green synthesized zinc oxide nanoparticle: Mechanism-based approach. Bioorg Chem 2020;94:103423.
9. Sofowora A, Ogunbodede E, Onayade A. The role and place of medicinal plants in the strategies for disease prevention. Afr J Tradit Complement Altern Med 2013;10:210-29.
10. Gupta PS, Patel S. *In vitro* antimitotic and cytotoxic potential of plant extracts: A comparative study of *Mucuna pruriens*, asteracantha *Longifolia* and *Sphaeranthus indicus*. Future J Pharm Sci 2020;6:115.
11. Kavitha KS, Baker S, Rakshith D, Kavitha HU, Yashwantha Rao HC, Harini BP, *et al*. Plants as green source towards synthesis of nanoparticles. Int Res J Biol Sci 2013;2:66-76.
12. Lampariello LR, Cortelazzo A, Guerranti R, Sticozzi C, Valacchi G. The magic velvet bean of *Mucuna pruriens*. J Tradit Complement Med 2012;2:331-9.
13. Mohapatra S, Ganguly P, Singh R, Katiyar CK. Estimation of levodopa in the unani drug *Mucuna pruriens* bak. And its marketed formulation by high-performance thin-layer chromatographic technique. J AOAC Int 2020;103:678-83.
14. Caronni S, Del Sorbo F, Barichella M, Fothergill-Misbah N, Denne T, Laguna J, *et al*. *Mucuna pruriens* to treat Parkinson's disease in low-income countries: Recommendations and practical guidelines from the farmer to clinical trials. Paving the way for future use in clinical practice. Parkinsonism Relat Disord 2024;124:106983.
15. Gupta S, Prem P, Sethy C, Shrivastava S, Singh M, Yadav P, *et al*. Exploring anticancer properties of medicinal plants against breast cancer by downregulating human epidermal growth factor receptor 2. J Agric Food Chem 2024;72:9717-34.
16. Agarwal H, Nakara A, Shanmugam VK. Anti-inflammatory mechanism of various metal and metal oxide nanoparticles synthesized using plant extracts: A review. Biomed Pharmacother 2019;109:2561-72.
17. Chandrasekaran AP, Sivamani S, Ranjithkumar V. Characterization of combined organic-inorganic acid-pretreated cassava stem. Int J Environ Sci Technol 2017;14:1291-6.
18. Mohan AC, Renjanadevi B. Preparation of zinc oxide nanoparticles and its characterization using scanning electron microscopy (SEM) and X-Ray diffraction (XRD). Procedia Technol 2016;24:761-6.
19. Tailor G, Chaudhay J, Verma D, Sarma BK. Microscopic study of zinc nanoparticles synthesised using thermosetting polymer. Appl Microsc 2019;49:20.
20. Jayachandran A, Aswathy TR, Nair AS. Green synthesis and characterization of zinc oxide nanoparticles using *Cayratia* Pedata leaf extract. Biochem Biophys Rep 2021;26:100995.
21. Abdelbaky AS, El-Mageed TA, Babalghith AO, Selim S, Mohamed AM. Green synthesis and characterization of ZnO nanoparticles using *Pelargonium odoratissimum* (L.) aqueous leaf extract and their antioxidant, antibacterial and anti-inflammatory activities. Antioxidants (Basel) 2022;11:1444.
22. Re R, Pellegrini N, Proteggente A, Pannala A, Yang M, Rice-Evans C. Antioxidant activity applying an improved ABTS radical cation decolorization assay. Free Radic Biol Med 1999;26:1231-7.
23. Shnawa BH, Jalil PJ, Al-Ezzi A, Mhamedsharif RM, Mohammed DA, Biro DM, *et al*. Evaluation of antimicrobial and antioxidant activity of zinc oxide nanoparticles biosynthesized with *ziziphus spina-christi* leaf extracts. J Environ Sci Health C Toxicol Carcinog 2024;42:93-108.
24. Karthik M, Ragunath C, Krishnasamy P, Paulraj DQ, Ramasubramanian V. Green synthesis of zinc oxide nanoparticles using *Annona muricata* leaf extract and its antioxidant and antibacterial activity. Inorg Chem Commun 2023;157:111422.
25. Marin-Flores CA, Rodríguez-Nava O, García-Hernández M, Ruiz-Guerrero R, Juárez-López F, Morales-Ramírez AD. Free-radical scavenging activity properties of ZnO sub-micron particles: Size effect and kinetics. J Mater Res Technol 2021;13:1665-75.
26. Kyene MO, Droepenu EK, Ayertey F, Yeboah GN, Archer MA, Kumadoh D, *et al*. Synthesis and characterization of ZnO nanomaterial from *Cassia sieberiana* and determination of its anti-inflammatory, antioxidant and antimicrobial activities. Sci Afr 2023;19:e01452.
27. Snezhkina AV, Kudryavtseva AV, Kardymon OL, Savvateeva MV, Melnikova NV, Krasnov GS, *et al*. ROS generation and antioxidant defense systems in normal and malignant cells. Oxid Med Cell Longev 2019;2019:6175804.